

Electronegativity Governs Enantioselectivity: Alkyl-Aryl Cross-Coupling with Fenchol-Based Palladium-Phosphorus Halide Catalysts

Roberto Blanco Trillo,^a Matthias Leven,^a Jörg M. Neudörfl,^a and Bernd Goldfuss^{a,*}

^a Department of Chemistry, Universität zu Köln, Greinstr. 4, 50939 Köln, Germany
Fax: (+49)-221-470-5057; e-mail: goldfuss@uni-koeln.de

Received: December 13, 2011; Revised: February 10, 2012; Published online: May 15, 2012

Supporting information for this article is available on the WWW under <http://dx.doi.org/10.1002/adsc.201100924>.

Abstract: A series of bulky, modular, monodentate, fenchol-based phosphites has been employed in an intramolecular palladium-catalyzed alkyl-aryl cross-coupling reaction. This enantioselective α -arylation of *N*-(2-bromophenyl)-*N*-methyl-2-phenylpropanamide is accomplished with $[\text{Pd}(\text{C}_3\text{H}_5)(\text{BIFOP-X})(\text{Cl})]$ as precatalysts, which are based on biphenyl-2,2'-bisfenchol phosphites (BIFOP-X, X = F, Cl, Br, etc.). The phosphorus fluoride BIFOP-F gives the highest enantioselectivity and good yields (64% *ee*, 88%). Lower selectivities and yields are found for BIFOP halides with heavier halogens (Cl: 74%, 47% *ee*, Br: 63%, 20% *ee*). NMR studies on catalyst com-

plexes reveal two equilibrating diastereomeric complexes in equal proportions. In all cases, the phosphorus-halogen moiety remains intact, pointing to its remarkable stability, even in the presence of nucleophiles. The increasing enantioselectivity of the catalysts with the phosphorus halide ligands correlates with the rising electronegativity of the halide (bromine < chlorine < fluorine), as can be rationalized from structural parameters and DFT computations.

Keywords: alpha-arylation; cross couplings; enantioselective catalysis; fenchol; palladium; phosphites

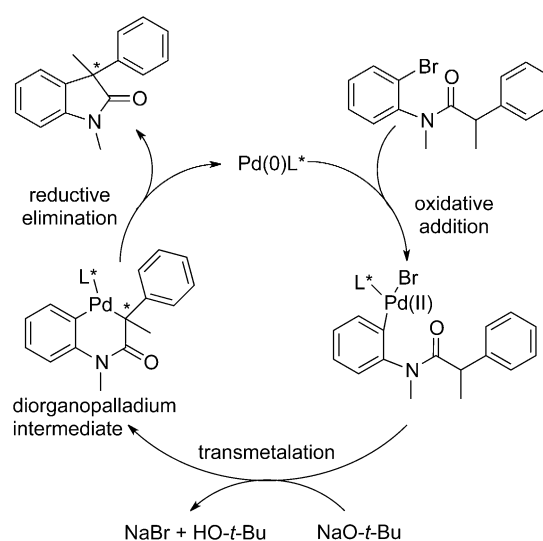
Introduction

Palladium-catalyzed cross-couplings^[1] are powerful tools for organic syntheses, for example, to generate quaternary carbon stereocenters.^[2] The normally complicated selective α -quaternation of carbonyl compounds can be effectively achieved *via* palladium catalyzed α -arylations (Scheme 1).^[3,4]

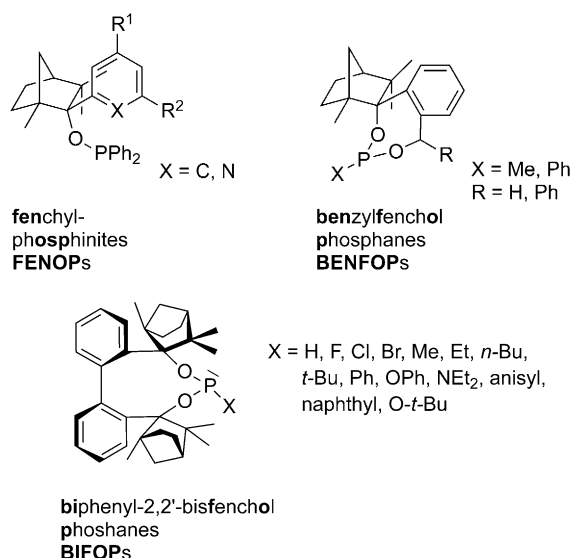
While a broad range of phosphines,^[5] N-heterocyclic carbenes (NHCs)^[6] or even secondary phosphine chlorides^[7] are used in Pd-catalyzed cross-couplings, a much more limited set of NHC and P ligands was applied in enantioselective α -arylations.^[3,4] The highest enantioselectivities were found for NHC ligands (up to 97% *ee*),^[8] with H₈-BINAP as the most successful P ligand up to 68% *ee* were achieved.^[9] The most selective monodentate P ligand accomplished 53% *ee*.^[5]

Fenchol-based^[10] (Scheme 2) reagents and catalysts were recently reported with applications in chiral organolithium aggregates^[11] and in enantioselective organozinc catalysts.^[12] The sterically highly hindered BIFOP ligands were employed in Cu-catalyzed 1,4-additions^[13a] and in Pd-catalyzed allylic substitu-

tions.^[13b] Surprisingly, the halogen phosphites BIFOP-Cl **2** and BIFOP-Br **3** were air-stable and proved to



Scheme 1. Catalytic cycle of an intramolecular, Pd-catalyzed α -arylation yielding chiral oxindoles.



Scheme 2. Fenchol-based P ligands, i.e., FENOPs, BENFOPs and BIFOPs.

be efficient ligands for the Pd catalyst, even in the presence of a nucleophilic reagent.

Herein, we discuss the synthesis and applications of fenchol-based P ligands (Scheme 2) for the enantioselective intramolecular Pd-catalyzed α -arylation and report the control of enantioselectivity by halide electronegativity in new halophosphite ligands.

Results and Discussion

Synthesis of Ligands

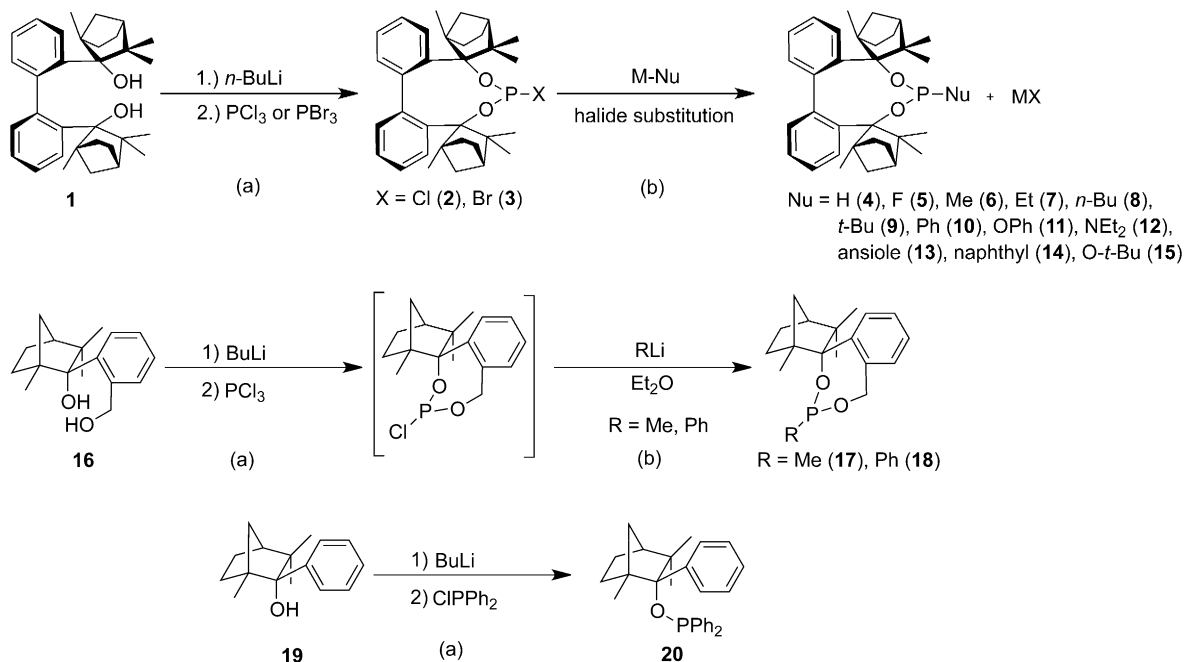
The biphenyl bisfenchol phosphines (BIFOPs) **1–15** were synthesized by lithiation of BIFOL **1** and subsequent reaction with PCl₃ or PBr₃ (Scheme 3).^[13] Instead of using PF₃, a halide substitution from BIFOP-Cl **2** with AgF was chosen in order to obtain the analogous fluorophosphite BIFOP-F **5**. All BIFOP halides (**2**, **3**, and **5**) are air stable and very reluctant to undergo reactions with various nucleophilic reagents (Table 1 and Table 3).^[13]

Different nucleophiles were used to substitute the chloride from **2** to get the ligands **4–15**. The same procedure was used to modify the Benfop **16** system (Scheme 3).

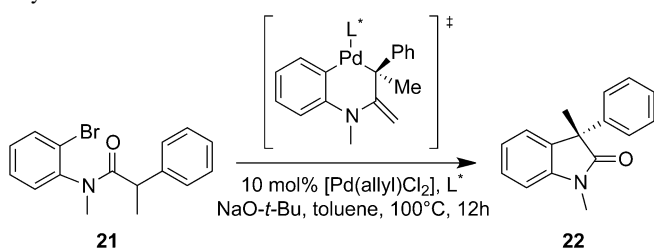
The BIFOP ligands were isolated in yields of 40–77%, while the BENFOP-based ligands could be isolated only with yields of 5 to 8%. These were stable at room temperature and mostly stable to hydrolysis. X-ray structures for all BIFOP derivatives (Figure 2 and Figure 3)^[13] reveal the rigid structure of the ligand-backbone with identical conformation for the biaryl-axis while BENFOP derivatives were only isolated as oils.

Enantioselective Intramolecular α -Arylation

The first set of experiments is performed with 10 mol% of [Pd(allyl)Cl]₂ and of the chiral ligand in



Scheme 3. Synthesis of the BIFOP- and BENFOP-based library. *Reaction conditions:* (a) lithiation followed by addition of PCl₃ or, respectively, PBr₃ (b) halide substitution.

Table 1. Pd-catalyzed cyclization of **21** via intramolecular α -arylation.^[a]

Ligand	Yield ^[b] [%]	<i>ee</i> ^[c] [%]
BIFOP-Cl ^[d] (2)	84	n.d.
BIFOP-H ^[d] (4)	86	>2 (<i>S</i>)
BIFOP-F ^[d] (5)	90	>2 (<i>S</i>)
BIFOP-Me ^[d] (6)	82	n.d.
BIFOP-Li (14)	0	–
BENFOP-Me (17)	33	7 (<i>R</i>)
BENFOP-Ph (18)	49	8 (<i>R</i>)
FENOP-Ph (20)	28	15 (<i>S</i>)

^[a] Reaction conditions: 10 mol% [Pd(allyl)Cl]₂, 10 mol% L*, 3 mL toluene, 100°C, 0.3 mmol amide, 0.9 mmol NaO-*t*-Bu, 100°C, 12 h.

^[b] Isolated yield.

^[c] Determinated by HPLC.

^[d] First heating of L* with [Pd(allyl)Cl]₂ for 5 h then the catalytic procedure.

toluene at 100°C for 12 h.^[8,9] These conditions give good yields (>84%) for all BIFOP-based ligands but hardly any enantioselectivities while the BENFOP (**17**, **18**) and FENOP (**19**) ligands give poor selectivities (Table 1). For the *in situ* generated lithium phosphite BIFOP-Li **14** no conversion is detected.

In order to obtain information on the formation of the *in situ* formed catalyst, NMR studies with BIFOP-Cl **2** and [Pd(allyl)Cl]₂ were carried out (Figure 1). Even after 1.5 h at 100°C a solution of BIFOP-Cl **2** and [Pd(C₃H₅)Cl]₂ in toluene still contains large amounts of free ligand **2** (³¹P NMR, δ =154.4, Figure 1). It takes as long as 5 h until all free BIFOP-Cl **2** is bound in the [Pd(**2**)(C₃H₅)Cl] complex (³¹P NMR, δ =137.3 and 138.0, Figure 1). Hence, this NMR analysis (Figure 1) shows that the bulky ligand reacts only slowly with the palladium species to form the catalyst, which is obviously caused by the high steric strain caused by the embedding fenchane units.^[13]

These NMR results are now employed to improve the catalytic procedure. For an optimized method, the catalysts are formed by equilibration for 5 h prior to catalysis. Indeed, both yields and enantioselectivities are substantially improved for all catalysts (Table 2). The best enantioselectivity was achieved with BIFOP-

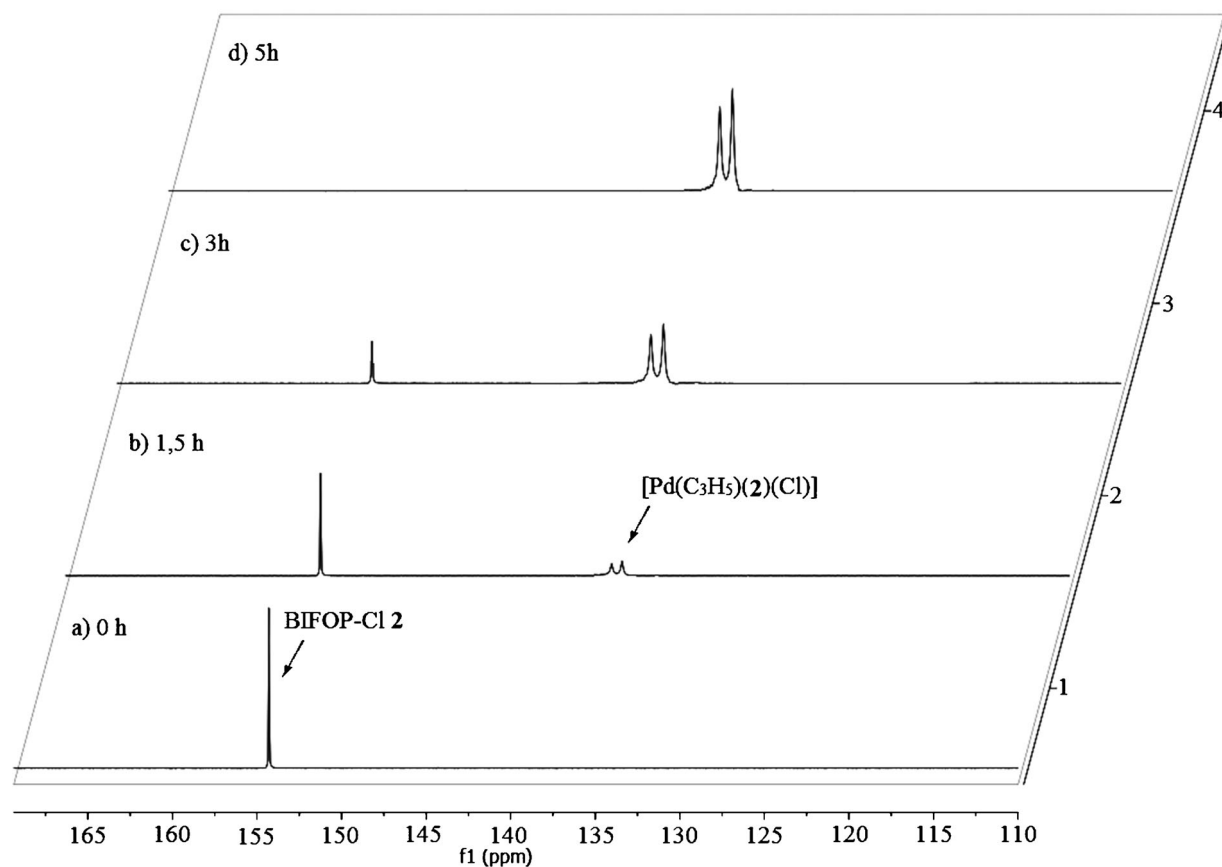


Figure 1. ³¹P NMR (CDCl₃; 125.5 MHz) of BIFOP-Cl **2** with [Pd(allyl)Cl]₂ after heating at 100°C for a) 0 h; b) 2.5 h; c) 3 h; d) 5 h, 0.038 mmol, 3 mL toluene.

Table 2. Optimized, Pd-catalyzed cyclization of **21** via intramolecular α -arylation.^[a]

Ligand	Yield ^[b] [%]	ee ^[c] [%]
BIFOP-Cl ^[d] (2)	74	47 (S)
BIFOP-Br ^[d] (3)	63	20 (S)
BIFOP-H ^[d] (4)	88	25 (S)
BIFOP-F ^[d] (5)	88	64 (S)
BIFOP-Me ^[d] (6)	63	13 (S)
BIFOP-Et ^[d] (7)	66	23 (S)
BIFOP- <i>n</i> -Bu ^[d] (8)	79	14 (S)
BIFOP- <i>t</i> -Bu ^[d] (9)	54	4 (S)
BIFOP-Ph ^[d] (10)	84	15 (S)
BIFOP-OPh ^[d] (11)	69	17 (S)
BIFOP-NEt ₂ ^[d] (12)	76	27 (S)
BIFOP-(2)-anisole ^[d] (13)	80	29 (S)
BIFOPLi (14)	0	–
BIFOP-O- <i>t</i> -Bu ^[d] (15)	70	9 (S)
BENFOP-Me (17)	91	7 (R)
BENFOP-Ph (18)	83	8 (R)
FENOP-Ph (20)	28	15 (S)

^[a] Reaction conditions: 10 mol% [Pd(allyl)Cl]₂, 10 mol% L*, 3 mL toluene, 100 °C, 5 h; then 0.3 mmol amide, 0.9 mmol NaO-*t*-Bu, 100 °C, 12 h.

^[b] Isolated yield.

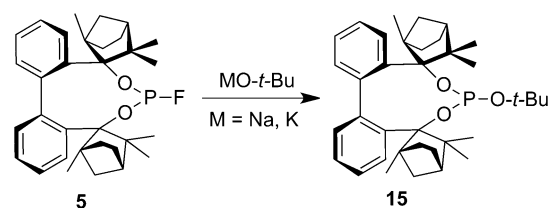
^[c] Determinated by HPLC.

^[d] First heating of L* with [Pd(allyl)Cl]₂ for 5 h then the catalytic procedure.

F 5 as ligand with 64% *ee* (Table 2). Remarkably, its activity and selectivity are significantly higher than for BIFOP-Cl **2** (47% *ee*), which itself is superior to BIFOP-Br **3** (20% *ee*, Table 2). In all cases, BIFOP derivatives were used, and the corresponding ligands could be recovered almost completely (80–90%) after the performed catalysis.

To test the stability of the BIFOP halides **2**, **3** and **5** against nucleophilic substitution with the employed base NaO-*t*-Bu, several experiments with different bases and solvents were performed (Table 3). All BIFOP halides have similar reactivity with the mentioned base and for the abridgement only BIFOP-F **5** as best ligand is listed (Table 3). The phosphorus fluoride **5** reacts with NaO-*t*-Bu neither under catalytic conditions (entry 1) nor in more polar solvents. Only with TMEDA as solvent and under high temperature for long time, is conversion of BIFOP-F **5** apparent (Table 3, entries 4 and 5). If BIFOP-O-*t*-Bu **15** was applied as ligand in the catalysis, only 9% *ee* (Table 2) are achieved. This catalytic performance of **15**, relative to BIFOP-F **5**, additionally proves that the phosphorus fluoride **5** is the active ligand system during the catalysis rather than the phosphite **15**.

In order to further improve the reaction conditions, a series of experiments was conducted in which the solvent and the amount of ligand are varied. For this purpose, the effects of different solvents are studied which were tested successfully previously in this catal-

Table 3. Stability of BIFOP-F **5** against NaO-*t*-Bu to form BIFOP-O-*t*-Bu **15**.

Entry	Reagent	Conditions	Conversion ^[a]
1	NaO- <i>t</i> -Bu	toluene, 100 °C, 24 h	–
2	NaO- <i>t</i> -Bu	MTBE, 50 °C, 24 h	–
3	NaO- <i>t</i> -Bu	THF, 60 °C, 12 h	–
4	NaO- <i>t</i> -Bu	TMEDA, 100 °C, 12 h	> 5%
5	NaO- <i>t</i> -Bu	TMEDA, 100 °C, 5 d	50%
6	KO- <i>t</i> -Bu	toluene, 100 °C, 12 h	decomposition

^[a] Determined by ³¹P NMR.

Table 4. Optimization of Pd source, solvent and temperature in the intramolecular α -arylation with BIFOP-F **5**.^[a]

BIFOP-F	Pd	Solvent	T [°C]	Yield ^[b]	ee ^[c]
10 mol%	[Pd(allyl)Cl] ₂	DME	100	76	56 (S)
10 mol%	[Pd(allyl)Cl] ₂	toluene	100	93	64 (S)
2.5 mol%	[Pd(allyl)Cl] ₂	DME	100	69	49 (S)
2.5 mol%	[Pd(allyl)Cl] ₂	toluene	100	93	57 (S)
10 mol%	[Pd(allyl)Cl] ₂	DME	50	50	50 (S)
10 mol%	[Pd(allyl)Cl] ₂	toluene	50	73	53 (S)
2.5 mol%	[Pd(allyl)Cl] ₂	DME	50	53	48 (S)
2.5 mol%	[Pd(allyl)Cl] ₂	toluene	50	93	45 (S)
10 mol%	Pd ₂ (dba) ₃	toluene	100	92	15 (S)
10 mol%	Pd(OAc) ₂	toluene	100	90	60 (S)

^[a] Reaction conditions: 10 mol% [Pd(allyl)Cl]₂, L*, 3 mL solvent, 100 °C, 5 h, then 0.3 mmol amide, 0.9 mmol NaO-*t*-Bu heat 12 h.

^[b] Isolated yield.

^[c] Determined by HPLC.

ysis.^[8] Two different catalyst loadings, i.e., 2.5 mol% and 10 mol%, at different temperatures, i.e., 50 °C and 100 °C, and different sources of palladium, i.e., ([Pd(allyl)Cl]₂), Pd₂(dba)₃ and Pd(OAc)₂) are employed. The results (Table 4) show that the combination of 10 mol% of [Pd(allyl)Cl]₂ and toluene as solvent at 100 °C gives the best selectivity and reactivity (88%, 64% *ee*, Table 4). This optimized procedure was employed in the foregoing screening of the ligands (Table 2).

Geometrical Comparisons of BIFOP Ligands

The results of the catalytic cross coupling (Table 2) indicate that enantioselectivity is strongly influenced by the ligand structures. Especially intriguing is the influ-

Table 5. Geometries based on X-ray structure of BIFOP-X systems and calculated *buried volumes*.^[a]

X	BAA [°] ^[b]	Angle sum at P [°] ^[c]	FAA-lp [°] ^[d]	FAA [°] ^[d]	V _{bur} at P (%) ^[a]
F (5)	−94.5	300.5	34.9	32.8	77.8
Cl (2) ^[e]	−91.3	305.2	38.9	37.1	44.2
Br (3) ^[e]	−91.7	306.6	38.9	36.9	46.8
H (4) ^[e]	−98.2	301.4	30.0	29.7	21.8
Ph (10)	−96.9	309.5	38.7	31.9	41.5
NEt ₂ (12) ^[e]	−91.1	309.2	35.8	35.1	31.5
OPh (11) ^[e]	−93.3	300.0	34.5	44.8	61.4
<i>n</i> -Bu (8) ^[e]	−98.2	303.6	31.4	34.5	17.7

^[a] The calculations used SambVca^[15] with the following parameters: radius of sphere, 3.5 Å; distance from sphere, 2.28 Å; mesh step, 0.05 Å.

^[b] Biaryl dihedral angle (BAA) between C1–C2–C3–C4 atoms in degrees.

^[c] Angle sum at phosphorus atom (pyramidal) in degrees.

^[d] Fenchyl-aryl dihedral angles (C1–C2–C3–O1) on the lone pair-side of phosphorus (FAA-lp) and at the substituent side (FAA) of the biaryl axis.

^[e] Already published, see ref.^[13]

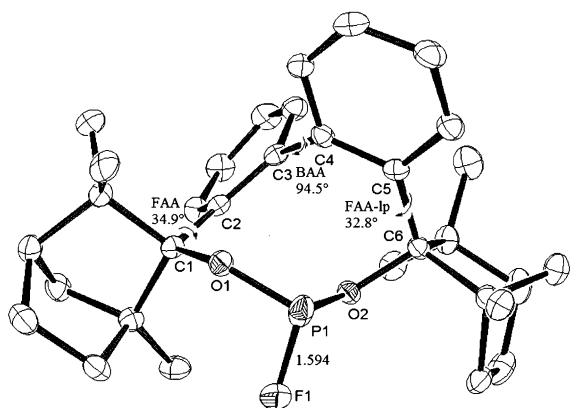


Figure 2. X-ray crystal structure of P-BIFOP-F **5**, with *Plus*-conformation of the biaryl axis, ellipsoids are shown with 50% probability.

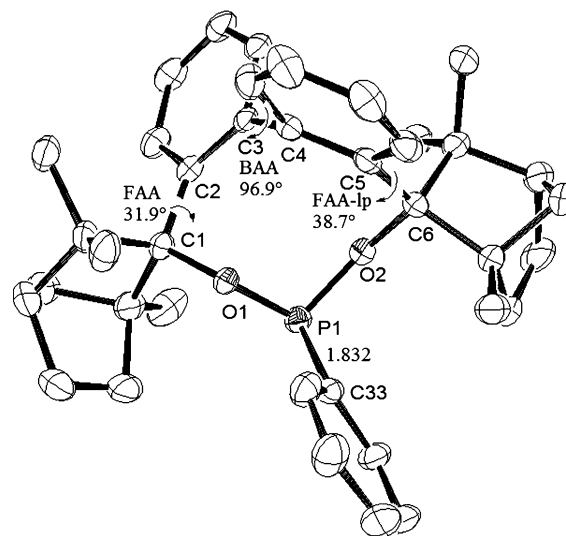


Figure 3. X-ray crystal structure of P-BIFOP-Ph **10**, with *Plus*-conformation of the biaryl axis, ellipsoids are shown with 50% probability.

ence of the halide in the phosphorus ligands BIFOP-Hal (Hal=Br, Cl, F) on the catalytic selectivities (Table 1). Hence, the crystal structures of all three BIFOP-halides **2**, **3**, **5** are compared to determine the structural effect of the halide. The geometries of all BIFOP derivatives are remarkable with respect to their biaryl angles (BAA), the fenchyl aryl angles (FAA, FAA-lp), the pyramidalities at the phosphorus atom as well as the positions of the phosphorus atom in the hydrophobic fenchane cavities (Table 5; Figure 2, Figure 3). All BIFOPs exhibit *Plus*-biaryl axes with dihedral angles varying from -91° to -99° (Table 5, Figure 2, Figure 3). The fenchyl aryl dihedral angles (FAA and FAA-lp) are crucial for the bite of the chiral diol and are between 30° and 40° , similar to fenchyl aryl angles previously analyzed in lithium fencholates.^[12] The difference between the two dihedral angles is a measure for the BIFOP asymmetry. The rate of the asymmetry is controlled by the pyramidal-

ity at the phosphorus atoms in BIFOPs, which distorts the inherent C_2 -symmetry of the biphenyl bisfenchol units towards C_1 -asymmetry. This is small for BIFOP-H **4** and all BIFOP halides (**2**, **3**, **5**), but large for the BIFOP-aryls (**10**, **13**) (Table 5). The phosphorus atoms, essential for coordination to transition metals, exhibit slightly different degrees of pyramidalities, the angle sums at phosphorus vary from 300° to 309° (Table 5).

To quantify the steric demand characterizing these ligands, the amount of volume of a sphere centered on the metal (*buried volume*^[14]), using SambVca was calculated.^[15] The volume of this sphere represents the space around the metal atom that must be shared by the different ligands upon coordination. To have

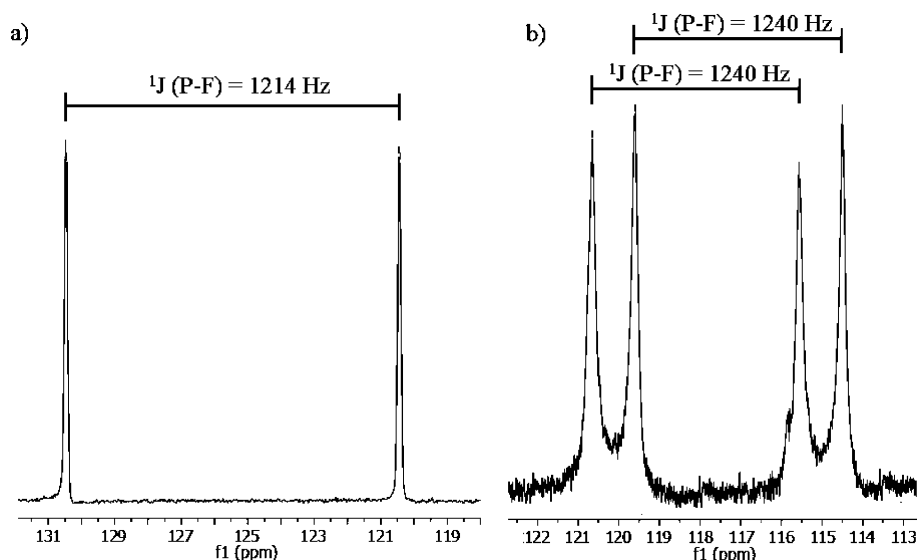


Figure 4. (a) ^{31}P NMR (125.5 MHz) of free ligand *P*-BIFOP-F **5**, $\delta = 125.5$ [$^1J(^{31}\text{P}-^{19}\text{F}) = 1214$ Hz]; (b) ^{31}P NMR (251 MHz) of the complex $[\text{Pd}(\text{C}_3\text{H}_5)(\mathbf{5})(\text{Cl})]$ **23**, $\delta = 117.5$ [$^1J(^{31}\text{P}-^{19}\text{F}) = 1240$ Hz].

an estimate of the bulkiness of the various ligands, the crystal structures of the free ligands are examined. The putative metal atom is positioned 2.28 Å from the coordinating P atom and the radius of the sphere was chosen to be 3 Å. The computation of the *buried volume* is presented in Table 5. Whereas BIFOP-Cl **2** and BIFOP-Br **3** exhibit a buried volume comparable to those of the prominent ligands TADDOL or BINAP, they exceed the *buried volume* of $\text{P}(t\text{-Bu})_3$ ($\%V_{\text{bur}} = 26.7$).^[14b] However, the steric demand of BIFOP-F **5** ($\%V_{\text{bur}} = 77.8$) exceeds that of the other ligands, its buried volume is among the largest reported so far for a monodentate ligand.^[14b] This high buried volume is caused by the short P–F distance, so that the size of the *chiral pocket* is reduced.^[17] This provides a rough explanation for the high enantioselectivity of BIFOP-F **5**, relative to the chloride **2** and the bromide **3**.

The relatively high enantioselectivity of the catalyst with ligand **5** is remarkable (Table 2), as the asymmetry of **5**, measured as the difference of its fenchyl-aryl angles, is rather small ($\Delta\text{FAA} = 2.1^\circ$, Table 5). In comparison to the other ligands **2–4** with similar asymmetry ($\Delta\text{FAA} = 0.3^\circ$ to 2.0°), the phosphorus atom in **5** is by far more encapsulated by the fenchane moieties (Table 5, 77.8%).

Characterization of Pd-BIFOP Halide Catalysts

To investigate the coordination behaviour of the bulky BIFOP halides **2** to palladium more in detail, Pd- π -allyl-complexes with ligands BIFOP-Cl **2**, BIFOP-Br **3** and BIFOP-F **5**, respectively, are studied by NMR spectroscopy. These complexes are obtained

by reaction of the ligands with 0.5 equivalents of the corresponding $[\text{Pd}(\text{allyl})\text{Cl}]_2$ dimer.^[18]

The ^{31}P NMR signal of free BIFOP-F **5** ($\delta = 125.5$, Figure 4, **a**) is shifted upfield in its $[\text{Pd}(\text{allyl})(\mathbf{5})\text{Cl}]$ -complex **23** ($\delta = 117.5$, Figure 4, **b**). The $^1J(^{31}\text{P}-^{19}\text{F})$ coupling of free **5** (1214 Hz) is increased to 1240 Hz in the Pd allyl complex **23** (Figure 4). This $^1J(^{31}\text{P}-^{19}\text{F})$ coupling proves that the P–F unit remains intact in the Pd complex **23**. The ^{31}P NMR upfield shift as well as the increased $^{31}\text{P}-^{19}\text{F}$ coupling in complex $[\text{Pd}(\text{allyl})(\mathbf{5})\text{Cl}]$ **23** relative to free BIFOP-F **5** parallels NMR spectroscopic investigations of Ru complexes.^[19]

The ^{31}P NMR-spectrum of the $\text{Pd}(\text{allyl})\text{Cl}$ -complex **23** (Figure 4) shows two additional resonances with almost equal intensities (1:0.9, Figure 4, **b**), which point to an equilibration of two diastereomers with *endo* (**23a**) and *exo* (**23b**) orientations of the allyl fragment (Figure 5).

Assignment of the *exo* **23a** and *endo* **23b** isomers by 2D NMR experiments was not possible because of the overlapping of the resonances arising from the protons of the fenchyl and terminal allyl groups. The $^1\text{H}-^1\text{H}$ NOESY and $^{19}\text{F}-^1\text{H}$ NOESY experiments show the absence of any cross-peaks between the two isomers. The $^{19}\text{F}-^1\text{H}$ NOESY experiment shows interaction between the P-bonded fluoride of both isomers and all allylic protons (Figure 6) while the $^1\text{H}-^{31}\text{P}$ correlation NMR spectrum shows cross-peaks between phosphorus and the central proton H_c ($\delta = 4.43$) but no interaction could be detected to both terminal allyl protons H_a ($\delta = 2.45$) and H_b ($\delta = 3.37$, Figure 7). In the $^1\text{H}-^{31}\text{P}$ correlation NMR spectrum two additional unusual high $^5J(\text{P}-\text{H})$ contacts can be observed between the phosphorus atom and a methyl group of

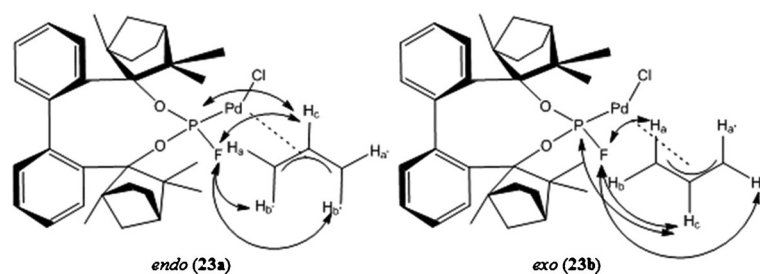


Figure 5. Equilibrating isomers of $[\text{Pd}(\text{allyl})(\mathbf{5})\text{Cl}]$ **23** with NOE interactions according to ^{19}F - ^1H NOESY and ^{31}P - ^1H correlation experiments.

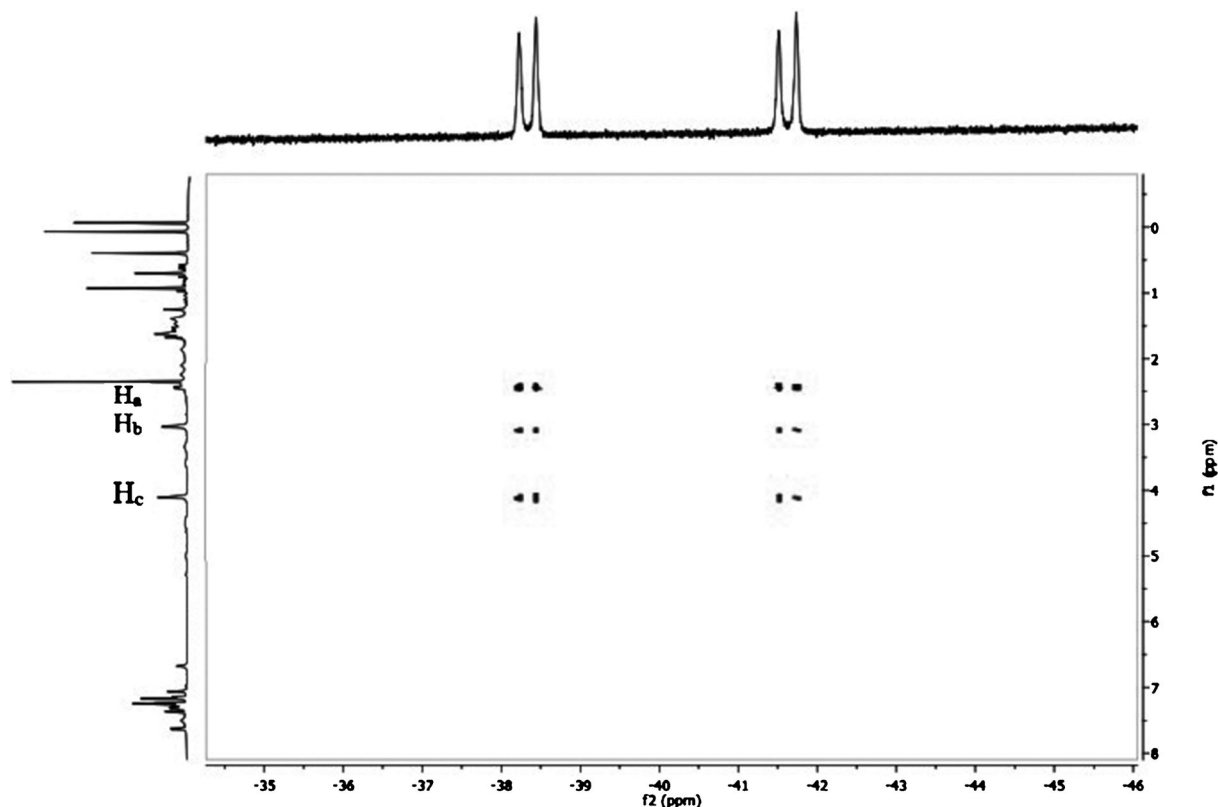


Figure 6. Relevant NOE contacts from the ^{19}F - ^1H NOESY experiment of the $[\text{Pd}(\text{allyl})(\mathbf{5})\text{Cl}]$ **23** isomers.

the fenchane backbone. Unreacted $[\text{Pd}(\text{C}_3\text{H}_5)(\text{Cl})_2]$ could not be detected [^1H NMR (CDCl_3) $\delta = 3.03$ (2H_{term} , d), 4.10 (2H_{term} , d), 5.45 (1H_{cen} , m)] in solution.

Hence, these NMR data prove the structure of complex $[\text{Pd}(\text{allyl})(\mathbf{5})\text{Cl}]$, which serves as a model for the active catalyst: BIFOP-F coordinates *via* the phosphorus atom to palladium, while the P-F unit remains intact.

A variable temperature NMR study of the complex $[\text{Pd}(\text{allyl})(\mathbf{5})\text{Cl}]$ **23**, between -40 and $+30^\circ\text{C}$, reveals that ligand **5** or complex **23** do not undergo any significant structural changes in solution, the spectra remain identical in this temperature range. A similar thermal stability is documented for $[\text{Pd}(\text{allyl})(\text{Cl})_2]$

complexes and bulky calyx[4]arene ligands.^[18c] DFT computations (Figure 8) show that the *endo* isomer of $[\text{Pd}(\text{allyl})(\mathbf{5})\text{Cl}]$ **23a** is slightly favoured by $0.6 \text{ kcal mol}^{-1}$ over *exo* **23b** (Figure 5). This is in good agreement with the equilibrium distribution of 1:0.9 observed by ^{31}P NMR spectroscopy (Figure 4). The preference of the *endo* isomer **23b** can be explained by its favoured *anti* *periplanar* orientation of the central proton of the allylic moiety relative to the halide atom bound to phosphorus atom (Figure 8).

Like the BIFOP-F **5** containing $[\text{Pd}(\text{C}_3\text{H}_5)(\mathbf{5})\text{Cl}]$ **23**, the analogous BIFOP-Cl **2** containing $[\text{Pd}(\text{C}_3\text{H}_5)(\mathbf{2})\text{Cl}]$ gives rise to two ^{31}P NMR signals at $\delta = 137.3$ and 138.0 for both its *endo* and *exo* diastereomers (Figure 9). Likewise, the BIFOP-Br **3** con-

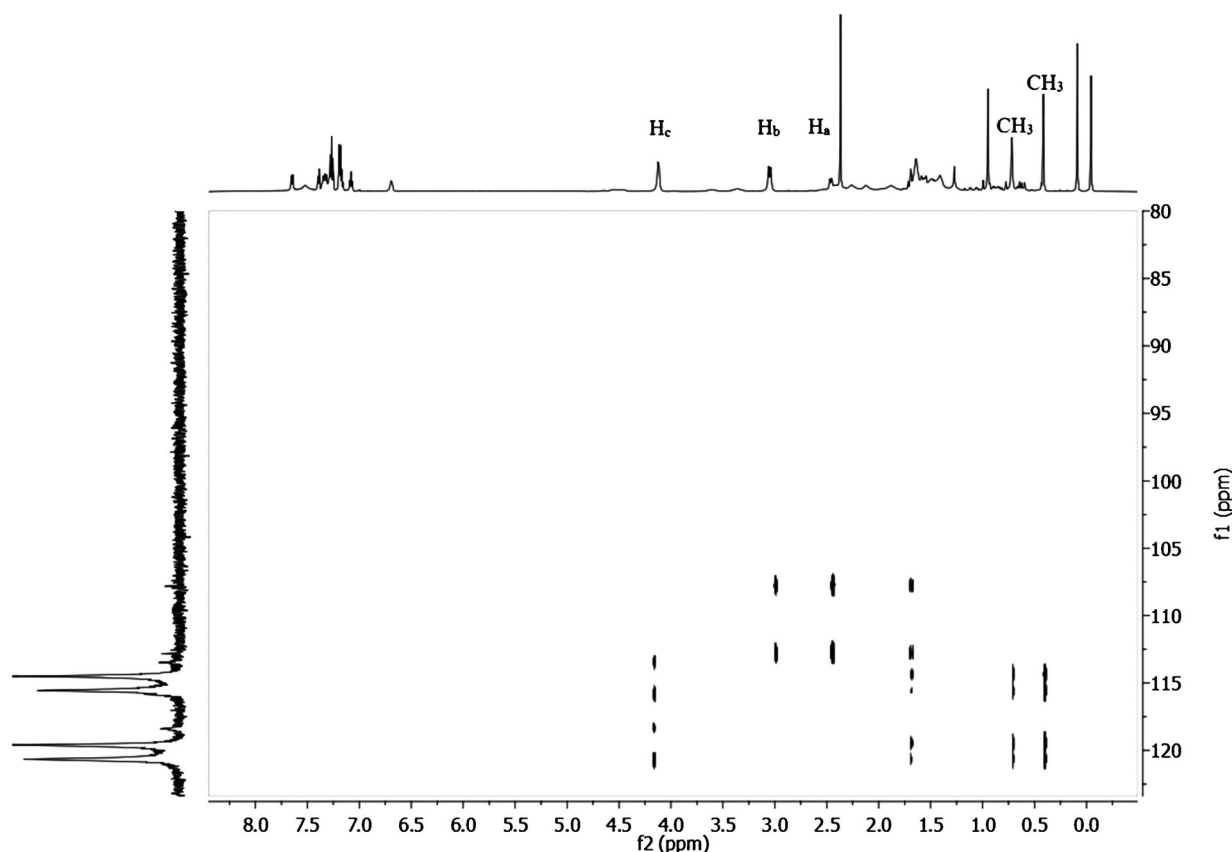


Figure 7. ^1H - ^{31}P correlation NMR spectra of the catalyst $[\text{Pd}(\text{allyl})(\mathbf{5})(\text{Cl})]$ **23**.

taining complex $[\text{Pd}(\text{C}_3\text{H}_5)(\mathbf{3})(\text{Cl})]$ shows two ^{31}P NMR signals $\delta = 119.9$ and 118.0 for the two diastereomers (Figure 9). Like the isomers **23a** and **23b**, the two resonances have almost equal intensities (1:0.9) and no significant change can be observed in the ^1H NMR spectrum or in the ^{31}P NMR spectrum upon variation of the temperature.

Origin of Enantioselectivity

The catalytic cyclizations of substrate **21** with BIFOP phosphite ($E_{\text{rel}} = 0.0 \text{ mol}^{-1}$) halides **2**, **3** and **5** show that yields and enantioselectivities are strongly affected by the type of halide present in the ligand and increase in the order $\text{Br} < \text{Cl} < \text{F}$: BIFOP-Br **3** (63% yield, 20% *ee*, *S*) BIFOP-Cl **2** (74% yield, 47% *ee*, *S*) and BIFOP-F **5** (88% yield, 64% *ee*, *S*, Table 2). To explore the origins of these intriguingly increasing enantioselectivities, the diorganopalladium intermediates $[\text{Pd}(\text{L})\text{R}_2]$, with $\text{R}_{1/2} = \mathbf{21}$, $\text{L} = \text{BIFOP-Hal}$, Scheme 1) were computationally analyzed as models for the transition structures of the enantioselective step, i.e., the foregoing transmetalation. T-shape geometries are well documented for such PdR_2L complexes.^[21] Hence, four $[\text{Pd}(\text{BIFOP-Hal})\text{R}_2]$ intermediates have to be considered with *trans* or *cis* P-Pd-aryl

arrangements and with *pro-S* or *pro-R* configured stereocenters. For each structure, the ONIOM (B3LYP/6-31G:UFF) two layer approach is employed to scan for the lowest energy conformation by rotation of the P-Pd axis in 10° steps. Subsequent geometry optimizations yield the four most stable isomers of the BIFOP-F **5** containing diorganopalladium intermediates $[\text{Pd}(\mathbf{21})(\mathbf{5})]$ **24** (Figure 10).

These computations show that the energetically most favoured intermediate is *pro-S* (**24a**), which competes with the *pro-R* intermediate (**24b**, Table 6). This *pro-S* preference agrees with the experimentally favoured *S*-configured product (Table 2). Furthermore, replacement of F by Cl or Br in BIFOP-Hal reduces the preference of *pro-S* vs. *pro-R* structures continuously: $E_{\text{rel}}(\text{F}) = 6.0 \text{ kcal mol}^{-1}$, $E_{\text{rel}}(\text{Cl}) = 1.4 \text{ kcal mol}^{-1}$, $E_{\text{rel}}(\text{Br}) = 0.1 \text{ kcal mol}^{-1}$ (Table 6). This is in agreement with the experimentally observed decreased enantioselectivities, i.e., F: 64% *ee* > Cl: 47% *ee* > Br: 20% *ee* for BIFOP-Hal, Table 1).

What are the origins for the *S*-enantiomeric product **22** yielding increasing enantioselectivities in the order $\text{Br} < \text{Cl} < \text{F}$ for BIFOP-X (X = halide) ligands? As it is apparent for the computed diorganopalladium intermediates $[\text{Pd}(\text{L})\text{R}_2]$, the energetic differentiation between the favoured *pro-S* and the disfavoured *pro-R* structures increases with decreasing phosphorus-

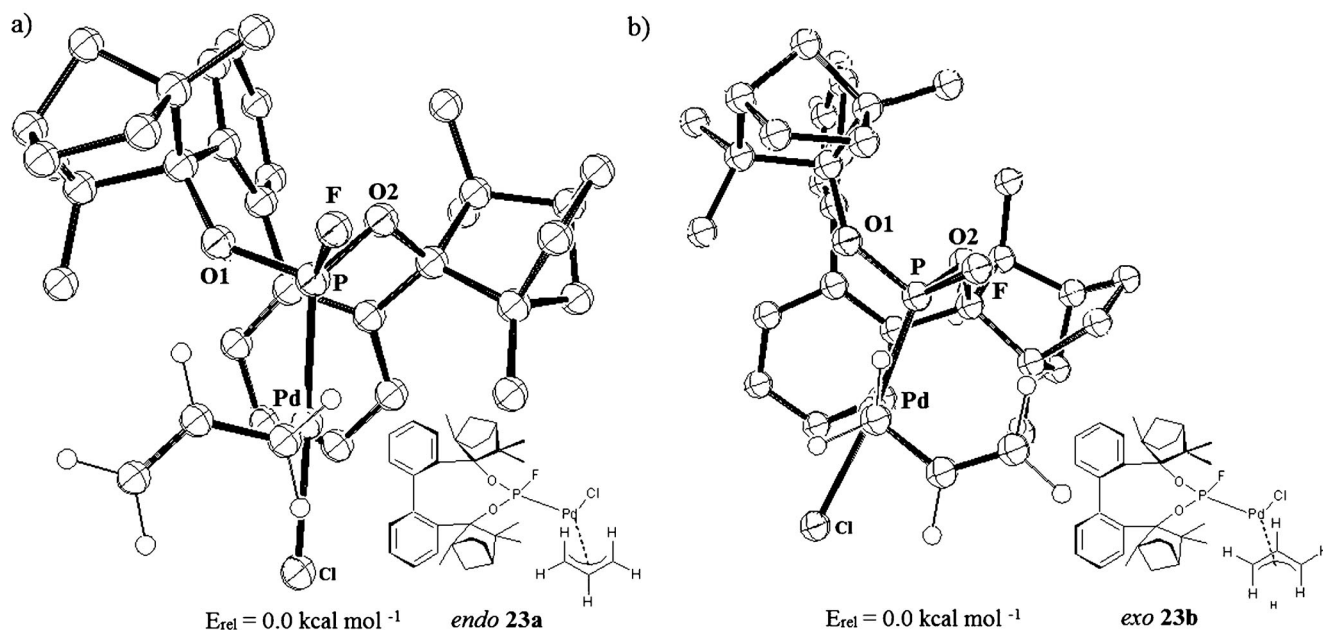


Figure 8. Computed structures of (a) the catalyst *exo*-[Pd(C₃H₅)(5)(Cl)] **23a** and (b) *endo*-[Pd(C₃H₅)(5)(Cl)] **23b** [BP86/def-SV(P)].

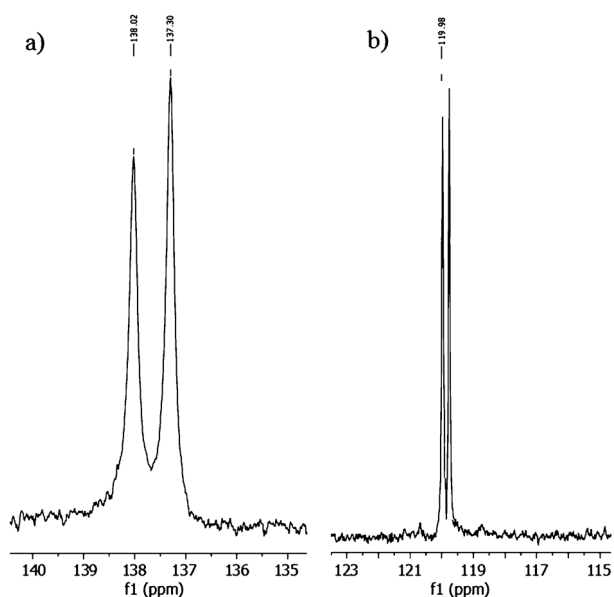


Figure 9. ³¹P NMR spectra (251 MHz, CDCl₃) of catalyst [Pd(C₃H₅)(**2**)(Cl)] (a) $\delta^{31}\text{P}$ = 137.3 and 138.0; (b) [Pd(C₃H₅)(**3**)(Cl)] $\delta^{31}\text{P}$ = 119.9 and 118.0.

palladium distances, i.e., *pro-S/R* from **3** (Br) 2.40/2.36 Å, over **2** (Cl) 2.39/2.35 Å to **5** (F) 2.37/2.32 Å (Table 6). Hence, in the order Br < Cl < F, the PdR₂ unit becomes more and more drawn into the chiral environment of the BIFOP halides. The distances between the halogen atoms (X) and the hydrogen atom H_(Cl) at the aryl *ortho*-position shorten with increasing electronegativity of X (Table 6, Figure 10). The closer

the contact to the chiral cavity, the higher is the energetic differentiation of *pro-S* and *pro-R* structures (Table 6). This agrees with the increasing experimental enantioselectivities in the order Br < Cl < F (Table 2). Bent's rule^[22] explains this electronegativity effect: As the more electronegative substituent induces more *p*-character at phosphorus in its bond to the P atom, more *s*-character, and hence a shorter bond distance results for the P–Pd coordination. The higher the electronegativity of the attached halogen atom, the shorter is the P–Pd bond.

Another proof for electronegativity-induced distortions is the pyramidity of the coordinating phosphorus atom, measured by its angle sum. X-ray crystal structures of the free BIFOP-X ligands show that this pyramidity increases with increasing electronegativity of the halide, in agreement with Bent's rule,^[22] i.e., angle sums are BIFOP-Br: 306.6° > BIFOP-Cl: 305.2° > BIFOP-F: 300.5° (Table 5). The same increased pyramidity at phosphorus with increased electronegativity of the attached halogen atom is apparent in the computed diorganopalladium intermediates (Figure 10, Table 6). Hence, the electronegativity of the halogen atoms attached to the coordinating P atom strongly influences the geometry of the intermediates and transition structures and governs the enantioselectivity of the catalyst.

Conclusions

New modular, fenchol-based, monodentate phosphine ligands provide in the Pd-catalyzed α -arylation of

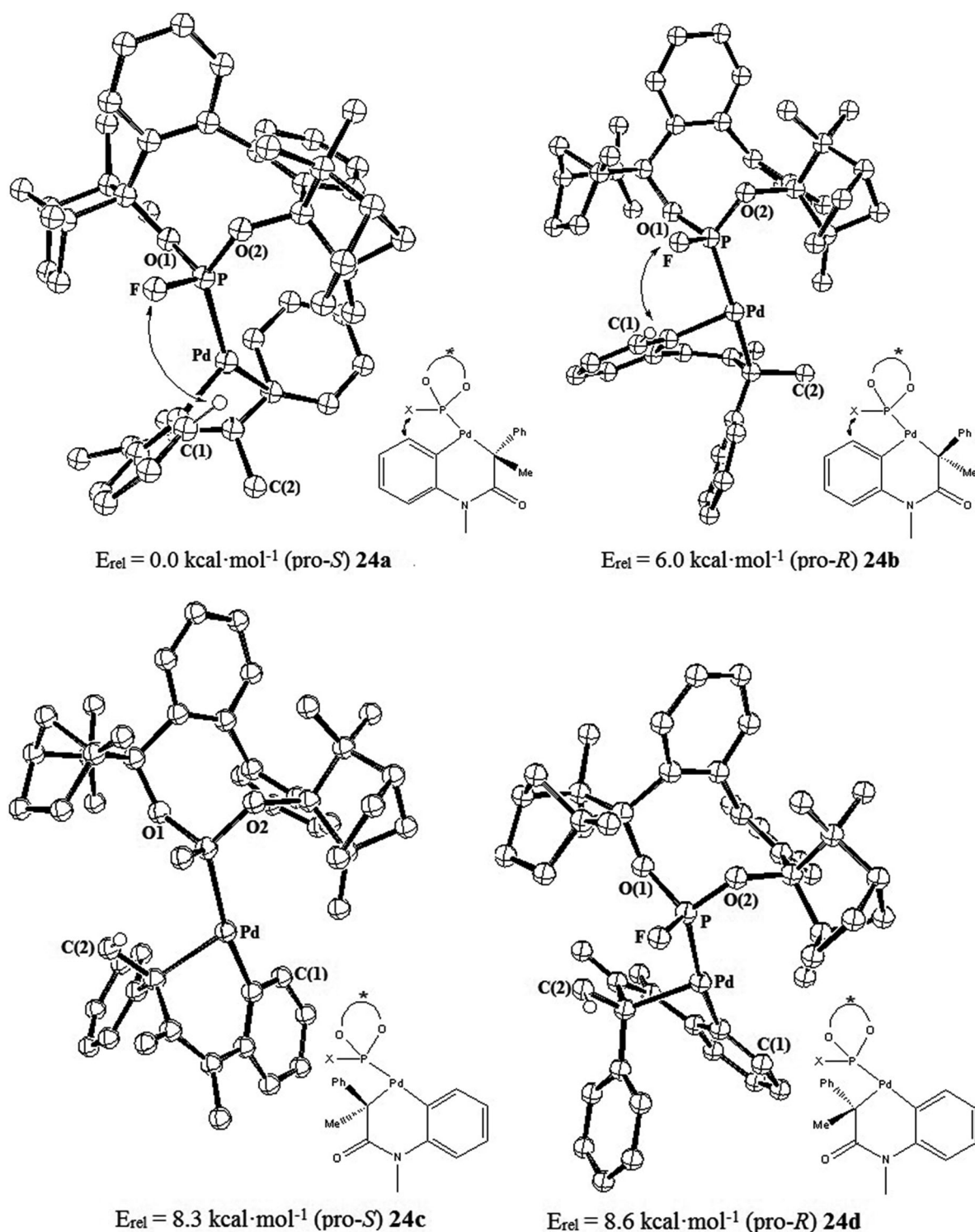


Figure 10. Computed structures of the diorganopalladium intermediate $[\text{Pd}(\mathbf{5})\text{R}_2]$ **24** [BP86/def-SV(P)]. The repulsive interaction between F and C(1)-H is shown for the two most stable structures (**24a** and **24b**, X = F).

amide **21** up to 88% yield and 64% *ee* (Table 2). Surprisingly, fluorophosphite BIFOP-F (**5**) is identified as the superior ligand, in spite of its potentially labile P–F function. Under the reaction conditions, the P–F group proves to be stable, even in the presence of nu-

cleophiles, which might be attributed to the strong steric shielding by the fenchane units. NMR experiments show that this shielding does not prevent coordination to palladium, which is necessary to form the active catalyst. The different electronegativities of the

Table 6. Computed relative energies and geometric parameters of diorgano palladium intermediates [Pd(2,3,5)R₂].^[a]

X	F (pro- <i>S</i> / <i>R</i>)	Cl (pro- <i>S</i> / <i>R</i>)	Br (pro- <i>S</i> / <i>R</i>)
E _{rel} ^[a]	6.0/0.0	1.4/0.0	0.1/0.0
P–Pd distance (Å) ^[a]	2.37/2.32	2.39/2.35	2.40/2.36
X–H _{C(1)} (Å) ^[a]	2.63/2.99	2.92/3.18	2.98/3.25
X–P–Pd (deg.) ^[a]	113.6/110.7	107.6/111.2	106.3/111.6
angle sum at P (deg.) ^[a]	302.4/301.0	306.8/304.8	308.5/306.2

^[a] E_{rel} in [kcal mol⁻¹] for the two most stable [Pd(L)R₂] structures [BP86/def-SV(P)]. D values show the geometric differences of pro-*S* and pro-*R* isomers.

halogen atoms in BIFOP-F, as well as its homologues BIFOP-Cl and BIFOP-Br, alter the geometries of ligands, catalysts, intermediates and transition structures to a different degree. Especially the shorter P–Pd contact, induced by the highly electronegative fluorine and the resulting more intensive substrate–ligand interaction, rationalizes the significantly higher enantioselectivity of BIFOP-F relative to its heavier homologues BIFOP-Cl and BIFOP-Br. This demonstrates the effect of electronegativity on the enantioselectivity in a Pd-catalyzed cross-coupling cyclization.

Experimental Section

BIFOP-Cl (2)

To a solution of 1.05 g (2.3 mmol) *P*-BIFOL **1** in 10 mL absolute THF, 2.81 mL (3 mmol) *tert*-butyllithium in hexanes (1.6M) were added slowly at –20°C. The mixture was stirred for 30 min, at –20°C then for 1 h at room temperature. After recooling to –20°C 0.3 mL (2.3 mmol) of freshly distilled PCl₃ were added slowly and the reaction mixture was stirred for 48 h at room temperature. Purification by flash chromatography (cyclohexane/Et₂O, 4:1) and recrystallization from Et₂O/CH₂Cl₂ furnished compound **1** as colourless crystals; yield: 0.76 g (1.5 mmol, 64%); mp 130.8°C; [α]_D²⁰: 74.31 (4.5 M in hexane). ³¹P NMR (125.5 MHz, CDCl₃): δ = 154.4; ¹H NMR (300 MHz, CDCl₃): δ = 0.07 (3H, s), 0.30 (3H, s), 0.65 (3H, s), 0.83 (3H, s), 1.10–1.61 (10H, m), 1.72 (3H, m), 2.24 (1H, d), 2.41 (1H, d), 2.48–2.67 (2H, m), 6.68 (1H, d), 6.97 (1H, t), 7.14–7.22 (2H, m), 7.50 (1H, d), 7.62 (1H, d); ¹³C NMR (CDCl₃): δ = 15.2, 16.1, 22.2, 22.7, 23.5, 23.9, 24.1, 25.4, 26.4, 26.7, 32.6, 38.3, 42.4, 42.6, 48.8, 49.0, 58.3, 58.7, 123.9, 125.8, 131.8, 133.9, 134.4, 143.8.

BIFOP-Br (3)

To a solution of 1.05 g (2.3 mmol) *P*-BIFOL **2** in 10 mL absolute THF, 2.81 mL (3 mmol) *tert*-butyllithium in hexanes (1.6M) were added slowly at –20°C. The mixture was stirred for 30 min, at –20°C then for 1 h at room temperature. After recooling to –20°C 0.3 mL (2.3 mmol) of freshly distilled PBr₃ were added slowly and the reaction mixture was stirred for 48 h at room temperature. Purification by flash chromatography (cyclohexane/Et₂O, 4:1) and recrystallization from Et₂O/CH₂Cl₂ furnished compound **3** as colour-

less crystals; yield: 0.78 g (1.6 mmol, 69%); mp 138.3°C; [α]_D²⁰: 18.29 (2.8 M in hexane). ³¹P NMR (125.5 MHz, CDCl₃): δ = 171.3; ¹H NMR (300 MHz, CDCl₃): δ = 0.89–0.68 (6H, m), 0.96 (3H, s), 1.00 (1H, t), 1.05 (3H, s), 1.17 (1H, t), 1.28 (3H, s), 1.43 (3H, s), 1.49–1.51 (1H, m), 1.85–1.66 (2H, m), 7.19–7.15 (1H, d), 7.37–7.26 (2H, m), 7.47 (1H, d); ¹³C NMR (75 MHz, CDCl₃): δ = 14.54, 15.68, 23.08, 24.35, 24.53, 25.79, 26.80, 27.34, 32.01, 33.07, 33.40, 37.39, 38.75, 42.88, 49.20, 51.34, 124.34, 126.22, 132.26, 134.28, 134.78, 144.22.

BIFOP-F (5)

To a solution of 1.0 g (2.2 mmol) *P*-BIFOP-Cl **2** in 15 mL absolute MeCN were added 792 mg (2.4 mmol) AgF. The mixture was stirred at room temperature for 12 h. Purification by flash chromatography (cyclohexane/Et₂O, 4:1) and recrystallization from Et₂O/CH₂Cl₂ furnished compound **5** as colourless crystals; yield: 0.79 g (1.7 mmol, 77%); mp 120.8°C; [α]_D²⁰: –48.53 (4.5 M in hexane). ³¹P NMR (125.5 MHz, CDCl₃): δ = 125.5 [¹J(P–F) = –1214 Hz]; ¹⁹F NMR (282.4 MHz, CDCl₃): δ = –53.1; ¹H NMR (300 MHz, CDCl₃): δ = 0.0 (3H, s, CH₃), 0.34 (3H, s, CH₃), 0.61 (3H, s, CH₃), 0.80 (3H, s, CH₃), 1.18–1.40 (6H, m), 1.45 (1H, m), 1.48 (2H, d), 1.50 (2H, s), 1.57 (2H, d), 2.08 (2H, m), 2.27 (1H, d, CH₃), 2.32 (1H, d, CH₃), 6.64 (1H, d), 6.66 (1H, t), 7.27–7.36 (2H, m), 7.41 (1H, t), 7.53 (1H, d); ¹³C NMR (75 MHz, CDCl₃): δ = 15.26, 23.93, 24.11, 25.37, 26.40, 32.65, 38.33, 42.46, 46.95, 48.77, 49.51, 123.93, 125.81, 131.81, 133.85, 133.87, 133.37, 143.80; X-ray crystal data: C₃₂H₄₀F₁O₂P₁; M_r = 506.61 g mol⁻¹; space group: P2₁2₁2₁; a = 8.1774(2), b = 13.9194(5), c = 23.1395(8) Å; V = 2633.84(15) Å³; Z = 4; ρ = 1.278 g mL⁻³; T = 100(2) K; λ = 0.71073; μ = 0.140 mm⁻¹; total reflections: 14335; unique reflections: 5764; observed: 4714 [I > 2σ(I)]; parameters refined: 331; R1 = 0.0473, wR2 = 0.1208; GOF = 1.042; H atoms bound to oxygen were refined, the positions of the H atoms bound to carbon were calculated. CCDC 865225 contains the supplementary crystallographic data for this paper. These data can be obtained free of charge from The Cambridge Crystallographic Data Centre via www.ccdc.cam.ac.uk/data_request/cif.

BIFOP-Me (6)

To a solution of 0.5 g (1.1 mmol) *P*-BIFOP-Cl **2** in 10 mL MTBE, 1.1 mL (1.1 mmol) methylolithium in hexanes were added slowly. The mixture was refluxed for 12 h, then the solvent was removed under vacuum. The residue was taken up in 10 mL of toluene, the suspension was stirred for 1 h

and then LiCl was filtered off through celite. The product **6** was obtained after crystallization in diethyl ether forming colourless needles; yield: 0.37 g, (0.9 mmol, 65%); mp 135.8°C; $[\alpha]_D^{20}$: 55.36 (4.5 M in hexane). ^{31}P NMR (125.5 MHz, CDCl_3): δ = 158.4 [$^2J(\text{P-H})$ = 11.5 Hz]; ^1H NMR (300 MHz, CDCl_3): δ = 0.81 (3H, s), 0.71 (6H, s), 1.11–0.97 (10H, m), 1.37–1.24 (4H, m), 1.71–1.56 (4H, m), 2.22–2.15 (2H, m), 2.39 (1H, d), 2.43 (1H, d), 2.85 (3H, d) 7.09–7.04 (2H, m), 7.15–7.11 (2H, m), 7.24 (1H, d), 7.28 (1H, t), 7.44 (2H, t), 7.51 (1H, d); ^{13}C NMR (75 MHz, CDCl_3): δ = 19.67, 21.22, 23.71, 30.05, 34.05, 42.53, 42.92, 45.29, 46.49, 49.20, 54.72, 61.36, 69.16, 71.21, 86.14, 91.36, 124.36, 124.77, 129.94, 133.22, 142.25, 146.38.

BIFOP-*t*-Bu (9)

To a solution of 0.5 g (1.1 mmol) BIFOP-Cl **2** in 10 mL MTBE, 1.9 mL (1.1 mmol) *tert*-butyllithium in hexanes (1.6M) were added slowly. The mixture was refluxed for 16 h, then the solvent was removed under vacuum. The residue was taken up in 20 mL of toluene, the suspension was stirred for 1 h and then LiCl was filtered off through celite. The product **9** was obtained after crystallization in $\text{Et}_2\text{O}/\text{CH}_2\text{Cl}_2$ forming colourless needles; yield: 0.36 g, (0.9 mmol, 76%); mp 139.9°C; $[\alpha]_D^{20}$: 69.53 (4.5 M in hexane). ^{31}P NMR (CDCl_3): δ = 174.2 [$^2J(\text{P-H})$ = 10.9 Hz]; ^1H NMR (300 MHz, CDCl_3): δ = 0.85–0.74 (6H, m), 1.29–0.98 (12H, m), 1.47–1.40 (4H, m), 1.67–1.54 (8H, m), 1.84–1.78 (4H, m), 2.03 (3H, d), 4.86 (2H, d), 7.09–7.04 (2H, m), 7.15–7.11 (2H, m), 7.24 (1H, d), 7.28 (1H, d), 7.44 (1H, d), 7.47 (1H, d); ^{13}C NMR (CDCl_3): δ = 13.61, 20.61, 21.37, 22.05, 22.37, 22.59, 23.43, 23.65, 26.88, 27.29, 27.64, 28.39, 29.63, 33.27, 38.72, 42.68, 45.10, 45.42, 49.43, 51.25, 52.25, 63.26, 106.10, 123.940, 124.16, 124.88, 125.04, 132.87, 133.01, 133.16, 133.68, 136.43, 145.83, 160.62.

BIFOP-Ph (10)

To a solution of 0.5 g (1.1 mmol) BIFOP-Cl **2** in 10 mL MTBE, 0.8 mL (1.5 mmol) phenyllithium in diethyl ether (2.0M) were added slowly. The mixture was refluxed for 12 h, then the solvent was removed under vacuum. The residue was taken up in 20 mL of toluene, the suspension was stirred for 1 h and then LiCl was filtered off through celite. The product **10** was obtained after crystallization in diethyl ether forming colorless needles; yield: 0.30 g (0.4 mmol, 40%); mp: 144.8°C; $[\alpha]_D^{20}$: -59.66 (4.5 M in hexane). ^{31}P NMR (125.5 MHz, CDCl_3): δ = 139.9 [$^2J(\text{P-H})$ = 11.4 Hz]; ^1H NMR (300 MHz, CDCl_3): δ = 0.31 (2H, s), 0.41 (3H, s), 0.61 (3H, s), 0.65 (3H, s), 0.79 (3H, s), 0.79 (3H, s), 0.86 (1H, m), 1.12–1.47 (8H, m), 1.61 (2H, m), 1.79 (3H, m), 2.03 (1H, m), 2.10 (1H, d), 2.50 (1H, d), 6.99 (1H, d), 7.06 (1H, dd), 7.10–7.24 (5H, m), 7.36 (1H, m), 7.70 (2H, m); ^{13}C NMR (75 MHz, CDCl_3): δ = 20.04, 20.59, 22.48, 23.65, 23.84, 36.04, 36.21, 37.66, 45.24, 45.93, 49.09, 50.05, 53.45, 54.84, 123.96, 124.29, 124.60, 125.15, 126.70, 128.70, 129.06, 130.13, 131.32, 133.80, 134.51, 135.29, 135.97, 144.27, 144.42, 146.44. X-ray crystal data: $\text{C}_{38}\text{H}_{45}\text{O}_2\text{P}_1$; M_r = 564.71 g mol^{-1} ; space group: $P2_12_12_1$; a = 11.5272(3), b = 13.2225(3), c = 19.9847(6) Å; V = 3046.04(14) Å³; Z = 4; ρ = 1.231 g mL^{-3} ; T = 100(2) K; λ = 0.71073; μ = 0.123 mm^{-1} ; total reflections: 20541; unique reflections: 6639; observed: 5577 [$I > 2s(I)$]; parameters refined: 376; $R1$ = 0.0393, $wR2$ = 0.0878; GOF =

1.029; H atoms bound to oxygen were refined, the positions of the H atoms bound to carbon were calculated. CCDC 865224 contains the supplementary crystallographic data for this paper. These data can be obtained free of charge from The Cambridge Crystallographic Data Centre via www.ccdc.cam.ac.uk/data_request/cif.

BIFOP-Anisole (13)

To a solution of 1.0 g (2.2 mmol) BIFOP-Cl **2** in 20 mL hexane, 1.4 mL (1.9 mmol) Li-anisole [formed from anisole and *tert*-butyllithium in hexanes (1.6M, 3 mmol)] were added slowly. The mixture was stirred for 5 h at room temperature and then refluxed for 12 h. The solvent was removed under vacuum. The residue was taken up in 20 mL of toluene, the suspension was stirred for 1 h and then LiCl was filtered off through celite. The product **13** was obtained after crystallization in $\text{Et}_2\text{O}/\text{CH}_2\text{Cl}_2$ forming colourless needles; yield: 0.21 g (0.4 mmol, 43%); mp 143.8°C; $[\alpha]_D^{20}$: -74.31 (4.5 M in hexane). ^{31}P NMR (125.5 MHz, CDCl_3): δ = 154.3 [$^2J(\text{P-H})$ = 6.5 Hz]; ^1H NMR (300 MHz, CDCl_3): δ = 0.00 (3H, s, CH_3), 0.32 (3H, s, CH_3), 0.67 (3H, s, CH_3), 0.85 (3H, s), 1.13–1.41 (7H, m), 1.47 (3H, m), 1.56 (2H, m), 1.62 (2H, m), 2.26 (1H, d), 2.43 (1H, d), 2.50–2.70 (2H, m), 3.08 (0H, s, OH), 6.71 (1H, dd, CH_{ar}), 6.85–6.94 (4H, m, CH_{ar}), 6.99 (1H, t, CH_{ar}), 7.52 (1H, t, CH_{ar}), 7.64 (1H, t, CH_{ar}); ^{13}C NMR (75 MHz, CDCl_3): δ = 19.54, 21.09, 22.48, 23.05, 23.49, 37.04, 36.21, 39.58, 45.34, 46.53, 48.29, 51.35, 53.85, 56.51, 123.96, 124.29, 124.60, 125.15, 126.70, 127.55, 128.66, 130.13, 131.39, 132.40, 134.51, 135.29, 137.63, 140.27, 143.02, 156.44.

BIFOP-O-*t*-Bu (15)

To a solution of 1.0 g BIFOP-Cl **2** (1.9 mmol) in 20 mL hexane, 1.4 mL (1.9 mmol) Li-anisole [formed from anisole and *tert*-butyllithium in hexanes (1.6M, 3 mmol)] were added slowly. The mixture was stirred for 5 days at 100°C and then refluxed for 12 h. The solvent was removed under vacuum. The residue was taken up in 20 mL of toluene, the suspension was stirred for 1 h and then LiCl was filtered off through celite. The product **15** was obtained after crystallization in diethyl ether forming colourless needles; yield: 0.763 g (74%). ^{31}P NMR (125.5 MHz, CDCl_3): δ = 176.2 [$^2J(\text{P-H})$ = 12.2 Hz]; ^1H NMR (CDCl_3): δ = 0.50 (1H, s), 0.69–0.64 (1H, m), 0.83 (3H, s), 0.94–0.92 (4H, m), 1.02–0.99 (4H, m), 1.08 (3H, s), 1.51–1.20 (8H, m), 1.80–1.62 (3H, m), 2.00–1.90 (1H, m), 2.20–2.14 (1H, m), 2.55–2.28 (2H, m), 2.79(1H, d), 7.08–7.00(3H, m), 7.32–7.15 (6H, m), 7.56 (1H, d), 7.67 (1H, d), 8.42 (1H, d); ^{13}C NMR (75 MHz, CDCl_3): δ = 15.30, 16.07, 18.22, 22.36, 23.17, 23.97, 24.15, 25.40, 26.44, 26.46, 33.03, 36.01, 38.37, 42.35, 42.49, 44.13, 48.81, 49.54, 52.12, 53.71, 123.84, 123.96, 124.38, 125.28, 125.84, 126.54, 129.37, 131.87, 133.03, 133.44, 133.69, 134.39, 135.16, 137.59, 143.17, 143.89.

Benfop-Me (17)

To a solution of 1.0 g (3.04 mmol) benzylfenchol in 10 mL THF at -78°C 4.2 mL (3.7 mmol) *n*-butyllithium in hexanes (1.6M) were added slowly. The mixture was stirred for 30 min at -78°C then for 1 h at room temperature. After cooling to 0°C 0.3 mL (2.3 mmol) of freshly distilled PCl_3

were added slowly and the reaction mixture was stirred for 16 h at room temperature. After cooling the mixture again to -78°C 2.4 mL (4.6 mmol, 1.2 equiv.) methyllithium (2M) were added dropwise. The solvent was removed under vacuum, the residue was taken up in 8 mL *n*-hexane and this mixture was stirred for 1 h. Filtration through celite to remove LiCl furnished compound **17** as a yellow oil 60 mg; yield: 0.86 mmol (5%); $[\alpha]_{\text{D}}^{20}$: -28.85 (4.5M in hexane). ^{31}P NMR (125.5 MHz, CDCl_3): $\delta = 139.2$ [$^2J(\text{P-H}) = 10.0$ Hz]; ^1H NMR (300 MHz, CDCl_3): $\delta = 0.50$ (3H, s, CH_3), 1.20 (3H, s, CH_3), 1.29 (12H, s, 4 CH_3), 1.37 (1H, dd, $^3J = 1.5$, 1.2 Hz, CH), 1.52–1.44 (1H, m, CH), 1.77–1.69 (3H, m, CH, CH_2), 2.20–2.10 (1H, m, CH), 2.43–2.39 (2H, m, CH_2), 6.99–6.93 (1H, t, H_{ar}), 7.19–7.13 (1H, t, H_{ar}), 7.50 u. 7.48 (1H, dd, $^3J = 1.2$, 1.5 Hz, H_{ar}), 7.19–7.13 (1H, t, H_{ar}), 8.34 u. 8.31 (1H, dd, $^3J = 1.5$, 1.2 Hz, H_{ar}), 10.43 (1H, br. s, NH); ^{13}C NMR (75 MHz, CDCl_3): $\delta = 15.54$, 17.72, 23.04, 25.26, 29.46, 30.69, 41.57, 46.49, 48.68, 52.58, 54, 87.57, 121, 122.76, 126.91, 128, 131, 139.30, 176.65; IR: $\nu = 3322$ (m); 2961 (s); 1650 (s); 1579 (s); 1519 (m); 1438 (m); 1307 (m); 1046 (w); 913 (w); 795 (m); 615 cm^{-1} (m).

BenfoP-Ph (18)

To a solution of 1.0 g (3.04 mmol) benzylfenchol in 10 mL THF at -78°C 4.2 mL (3.7 mmol) *n*-butyllithium in hexanes (1.6M) were added slowly. The mixture was stirred for 30 min at -78°C then for 1 h at room temperature. After re-cooling to 0°C 0.3 mL (2.3 mmol) of freshly distilled PCl_3 were added slowly and the reaction mixture was stirred for 16 h at room temperature. After cooling the mixture again to -78°C 2.4 mL (4.6 mmol, 1.2 equiv.) phenyllithium (2M) were added dropwise. The solvent was removed under vacuum, the residue was taken up in 8 mL *n*-hexane and this mixture was stirred for 1 h. Filtration through celite to remove LiCl furnished compound **18** as a yellow oil; yield: 71 mg (0.93 mmol, 8%); $[\alpha]_{\text{D}}^{20}$: -35.38 (4.5M in hexane). ^{31}P NMR (125.5 MHz, CDCl_3): $\delta = 129.0$; ^1H NMR (300 MHz, CDCl_3): $\delta = 0.74$ (3H, s, CH_3), 0.82 (3H, s, CH_3), 1.09 (3H, s, CH_3), 1.91 (1H, td, $^3J = 1.5$, 1.2 Hz, CH), 1.20 (2H, d), 1.32 (1H, m), 1.54 (1H, d), 1.79 (1H, d), 1.92 (2H, m), 4.97 (2H, dd), 7.25 (2H, m), 7.37 (2H, m); ^{13}C NMR (75 MHz, CDCl_3): $\delta = 17.76$, 23.07, 25.24, 29.47, 30.63, 41.54, 46.13, 48.61, 52.54, 71.60, 98.86, 120.58, 125.17, 125.83, 126.65, 128.47, 128.72, 133.64, 133.9, 140.5, 141.7; IR: $\nu = 2956$ (m), 2926 (s), 2870 (m), 2843 (w), 1458 (s), 1435 (s), 1519 (m), 1438 (m), 1112 (m), 1056 (s), 1026 (m), 1010 (w), 956 (w), 748 (s), 719 (w), 696 cm^{-1} (m).

BIFOP-F-Palladium Allylate (21)

38.0 mg (0.075 mmol) BIFOP-F **5** and 13.8 mg (0.038 mmol) allylpalladium chloride dimer were stirred in 3 mL toluene and heated at 100°C for 5 h. A yellow solid precipitated from the solution. The solid was washed with Et_2O and then dried under vacuum. Recrystallization from CH_2Cl_2 gave **21** as a yellow solid; yield: 36.0 mg (0.052 mmol). ^{31}P NMR (251 MHz, CDCl_3): $\delta = 118.1$ and 117.0 [$^1J(\text{P-F}) = -1240$ Hz]; ^{19}F (564.8 MHz, CDCl_3): $\delta = -40.0$; ^1H NMR (600 MHz, CDCl_3): $\delta = 0.06$ (3H, s, CH_3), 0.40 (3H, s, CH_3), 0.70 (3H, s, CH_3), 0.93 (3H, s, CH_3), 1.25 (2H, s, CH_2), 1.39 (3H, m), 1.47 (2H, m), 1.57 (3H, m), 1.62–1.70 (6H, m), 2.45 (1H, d, allyl), 3.37 (1H, d, allyl), 4.43 (1H, s, allyl),

6.68 (1H, d), 7.06 (1H, t), 7.30–7.34 (2H, m), 7.38 (1H, t), 7.63 (1H, d); ^{13}C NMR (150 MHz, CDCl_3): $\delta = 19.28$, 23.34, 23.90, 28.11, 28.66, 29.79, 36.38, 45.28, 45.44, 48.62, 48.85, 50.39, 52.00, 53.40, 74.93, 106.24, 124.81, 126.91, 128.53, 128.64, 133.73, 137.73, 140.83, 141.96.

BIFOP-Cl-Palladium Allylate (22)

39.2 mg (0.075 mmol) BIFOP-Cl **2** and 13.8 mg (0.038 mmol) allylpalladium chloride dimer were stirred in 3 mL toluene and heated at 100°C for 5 h. A yellow solid precipitated from solution. The solid was washed with Et_2O and then dried under vacuum. Recrystallization from CH_2Cl_2 gave **22** as a yellow solid; yield: 51 mg (0.068 mmol). ^{31}P NMR (251 MHz, CDCl_3): $\delta = 138.0$ and 137.3 ; ^1H NMR (600 MHz, CDCl_3): $\delta = 0.07$ (3H, s, CH_3), 0.42 (3H, s, CH_3), 0.73 (3H, s, CH_3), 0.95 (3H, s, CH_3), 1.29 (2H, s, CH_2), 1.53 (3H, m), 1.61 (5H, m), 1.68–1.78 (6H, m), 2.49 (1H, d, allyl), 3.41 (1H, d, allyl), 4.50 (1H, s, allyl), 6.68 (1H, d), 7.06 (1H, t), 7.30–7.34 (2H, m), 7.38 (1H, t), 7.63 (1H, d); ^{13}C NMR (150 MHz, CDCl_3): $\delta = 19.48$, 21.61, 23.10, 24.18, 28.03, 28.59, 28.39, 37.39, 42.54, 48.68, 50.32, 52.24, 63.18, 125.36, 126.29, 127.22, 128.30, 128.49, 128.84, 129.10, 129.78, 131.02, 133.90, 137.39, 141.19, 142.92.

BIFOP-Br-Palladium Allylate (23)

42.6 mg (0.075 mmol) BIFOP-Br **3** and 13.8 mg (0.038 mmol) allylpalladium chloride dimer were stirred in 3 mL toluene and heated at 100°C for 5 h. A yellow solid precipitated from solution. The solid was washed with Et_2O and then dried under vacuum. Recrystallization from CH_2Cl_2 gave **23** as a yellow solid; yield: 38.5 mg (0.055 mmol). ^{31}P NMR (251 MHz, CDCl_3): $\delta = 119.9$ and 119.3 ; ^1H NMR (600 MHz, CDCl_3): $\delta = 0.08$ (3H, s, CH_3), 0.44 (3H, s, CH_3), 0.77 (3H, s, CH_3), 0.99 (3H, s, CH_3), 1.23 (2H, s, CH_2), 1.41 (3H, m), 1.49 (2H, m), 1.63 (3H, m), 1.71–1.82 (6H, m), 2.52 (1H, d, allyl), 3.49 (1H, d, allyl), 4.49 (1H, s, allyl), 6.73 (1H, d), 7.09 (1H, t), 7.32–7.36 (2H, m), 7.39 (1H, t), 7.67 (1H, d); ^{13}C NMR (150 MHz, CDCl_3): $\delta = 19.40$, 23.49, 23.97, 28.28, 28.79, 29.84, 36.46, 45.32, 45.60, 48.49, 48.97, 50.60, 51.99, 53.53, 74.01, 106.41, 124.97, 127.10, 128.74, 128.80, 133.92, 137.88, 140.95, 142.18.

Asymmetric Synthesis of (S)-1,3-Dimethyl-3-phenylindolin-2-one (20)

$\text{Pd}(\text{allyl})\text{Cl}]_2$ (5 mol%), ligand (10 mol%), $\text{NaO-}t\text{-Bu}$ (43 mg, 0.45 mmol, 3 equiv.) and the starting material (0.3 mmol) were combined with 3 mL toluene and stirred at 100°C until all starting material was consumed (GC/MS). After completion the mixture was filtered through a short plug of silica, diluted with 50 mL EtOAc and the solvents were evaporated. The crude material was dissolved in a small amount of CH_2Cl_2 , adsorbed on silica and purified by flash chromatography (silica, pentane/ $\text{EtOAc} = 10:1$) as a pale oil; R_f (pentane/ EtOAc , 5:1): 0.26. ^1H NMR (300 MHz, CDCl_3): $\delta = 1.81$ (s, 3H), 3.25 (s, 3H), 6.93 (d, $J = 7.8$ Hz, 1H), 7.11 (dt, $J = 7.5$ Hz, $J = 1.0$ Hz, 1H), 7.19–7.36 (m, 7H); ^{13}C NMR (75 MHz, CDCl_3): $\delta = 23.7$, 26.4, 52.1, 108.2, 122.7, 124.1, 126.6, 127.1, 128.0, 128.4, 134.7, 140.7, 143.2, 179.3; GC-MS (method 50–300M): $t_R = 9.31$ min; MS-EI: m/z (%) = 237 (96), 222 (100), 207 (12), 194 (20), 165 (12), 152 (9); ESI-

MS: $m/z=260.1040$, calcd. for $[C_{16}H_{15}NONa]^+$: 260.1046. The enantiomeric excess was determined by HPLC analysis with a chiral column (Chiral Diacel OD-H; 25 cm \times 0.46 cm; hexane/*i*-PrOH=98/2, UV-vis: $\lambda=254$ nm). The analysis gave two separate peaks (flow rate: 1.0 mL min⁻¹): $t_r=12.86$ min [*S*(-)-**20a**], 15.36 min [*R*(+)-**20b**].

Acknowledgements

We are grateful to the Fonds der Chemischen Industrie for financial support. We also thank the Deutsche Forschungsgemeinschaft (DFG) for funding as well as Bayer AG, BASF AG, Wacker AG, Evonic AG, Raschig GmbH, Symrise GmbH, Solvay GmbH and the OMG group for generous support. We thank the Regionales Rechenzentrum zu Köln (RRZK), especially Dr. Lars Packschies, for the maintenance of the HPLC systems and Prof. Dr. Luigi Cavallo for the fast addition of the Br parameters to the SambVca database.

References

- [1] a) F. Diederich, P. J. Stang, (Eds.), *Metal-catalyzed Cross-coupling Reactions*, Wiley-VCH, Weinheim, **1998**; b) T. Hayashi, in: *Comprehensive Asymmetric Catalysis*, Vol. 1, Springer, Heidelberg, **1999**.
- [2] a) U. Christmann, R. Vilar, *Angew. Chem.* **2005**, *117*, 370; *Angew. Chem. Int. Ed.* **2005**, *44*, 366; b) T. E. Barder, S. D. Walker, J. R. Martinelli, S. L. Buchwald, *J. Am. Chem. Soc.* **2005**, *127*, 4685.
- [3] a) D. A. Culkin, J. F. Hartwig *Organometallics* **2004**, *23*, 3398; b) G. Mann, Q. Shelby, A. H. Roy, J. F. Hartwig, *Organometallics* **2003**, *22*, 2775; c) Q.-S. Hu, Y.; Lu, Z.-Y. Tang, H.-B. Yu, *J. Am. Chem. Soc.* **2003**, *125*, 2856.
- [4] In the last few years new catalysts were developed which were able to activate less reactive aryl chlorides: a) B. C. Hamann, J. F. Hartwig, *J. Am. Chem. Soc.* **1997**, *119*, 12382; b) H. Muratake, M. Natsume, *Tetrahedron Lett.* **1997**, *38*, 7581; c) M. Palucki, S. L. Buchwald, *J. Am. Chem. Soc.* **1997**, *119*, 11108; d) T. Satoh, Y. Kawamura, M. Miura, M. Nomura, *Angew. Chem.* **1997**, *109*, 1820; *Angew. Chem. Int. Ed. Engl.* **1997**, *36*, 1740; e) K. H. Shaughnessy, B. C. Hamann, J. F. Hartwig, *J. Org. Chem.* **1998**, *63*, 6546; f) M. Kawatsura, J. F. Hartwig, *J. Am. Chem. Soc.* **1999**, *121*, 1473; g) J. M. Fox, X. H. Huang, A. Chieffi, S. L. Buchwald, *J. Am. Chem. Soc.* **2000**, *122*, 1360.
- [5] A. C. Frisch, N. Shaikh, A. Zapf, M. Beller, *Angew. Chem.* **2002**, *114*, 4218; *Angew. Chem. Int. Ed.* **2002**, *41*, 4056.
- [6] A. C. Frisch, F. Rataboul, A. Zapf, M. Beller, *J. Organomet. Chem.* **2003**, *687*, 403.
- [7] L. Ackermann, A. R. Kapdi, C. Schulzke, *Org. Lett.* **2010**, *12*, 2298.
- [8] a) F. Glorius, S. Würtz, C. Lohre, R. Fröhlich, K. Bergander, *J. Am. Chem. Soc.* **2009**, *131*, 8344; b) J. F. Hartwig, S. Lee, *J. Org. Chem.* **2001**, *66*, 3402; c) D. J. Spiegelvogel, S. L. Buchwald, *J. Am. Chem. Soc.* **2002**, *124*, 3500.
- [9] a) I. D. Hills, G. C. Fu, *Angew. Chem.* **2003**, *115*, 4051; *Angew. Chem. Int. Ed.* **2003**, *42*, 3921; b) T. Arao, K. Kondo, T. Aoyama, *Chem. Pharm. Bull.* **2006**, *54*, 1743; c) S. Lee, J. F. Hartwig, *J. Org. Chem.* **2001**, *66*, 3402.
- [10] a) D. Lange, J. M. Neudörfl, B. Goldfuss, *Tetrahedron* **2006**, *62*, 3704; b) F. Soki, J.-M. Neudörfl, B. Goldfuss, *Tetrahedron* **2005**, *61*, 10449; c) B. Goldfuss, T. Löschmann, F. Rominger, *Chem. Eur. J.* **2001**, *7*, 2028; d) B. Goldfuss, F. Rominger, *Tetrahedron* **2000**, *56*, 881; e) B. Goldfuss, E. Eisenträger, *Aust. J. Chem.* **2000**, *53*, 209; f) B. Goldfuss, T. Löschmann, F. Rominger, *Chem. Eur. J.* **2004**, *10*, 5422.
- [11] a) M. Steigelmann, Y. Nisar, F. Rominger, B. Goldfuss, *Chem. Eur. J.* **2002**, *8*, 5211; b) B. Goldfuss, M. Steigelmann, F. Rominger, *Eur. J. Org. Chem.* **2000**, 1785; c) B. Goldfuss, M. Steigelmann, *J. Mol. Model.* **2000**, *6*, 166; d) B. Goldfuss, M. Steigelmann, S. I. Khan, K. N. Houk, *J. Org. Chem.* **2000**, *65*, 77; e) B. Goldfuss, S. I. Khan, K. N. Houk, *Organometallics* **1999**, *18*, 2927.
- [12] a) M. Leven, N. E. Schlörer, J. M. Neudörfl, B. Goldfuss, *Chem. Eur. J.* **2010**, *16*, 13443; b) A. Gliga, H. Klare, M. Schumacher, F. Soki, J. M. Neudörfl, B. Goldfuss, *Eur. J. Org. Chem.* **2011**, 256–263; c) B. Goldfuss, *Synthesis* **2005**, 2271; d) B. Goldfuss, M. Steigelmann, T. Löschmann, G. Schilling, F. Rominger, *Chem. Eur. J.* **2005**, *11*, 4019; e) B. Goldfuss, M. Steigelmann, F. Rominger, H. Urtel, *Chem. Eur. J.* **2001**, *7*, 4456; f) B. Goldfuss, M. Steigelmann, F. Rominger, *Angew. Chem.* **2000**, *112*, 4299; *Angew. Chem. Int. Ed.* **2000**, *39*, 4133.
- [13] a) B. Goldfuss, T. Kop-Weiershausen, J. Lex, J.-M. Neudörfl, *Beilstein J. Org. Chem.* **2005**, *1*, 6; b) B. Goldfuss, T. Löschmann, T. Kop-Weiershausen, J. Neudörfl, F. Rominger, *Beilstein J. Org. Chem.* **2006**, *2*, 7.
- [14] a) R. Dorta, E. D. Stevens, N. M. Scott, C. Costabile, L. Cavallo, C. D. Hoff, S. P. Nolan, *J. Am. Chem. Soc.* **2005**, *127*, 2485; b) H. Clavier, S. P. Nolan, *Chem. Commun.* **2010**, *46*, 841–861; c) A. Poater, B. Cosenza, A. Correa, S. Guidice, F. Ragone, V. Scarano, L. Cavallo, *Eur. J. Inorg. Chem.* **2009**, 1759.
- [15] For details see: <http://www.molnac.unisa.it/OM-tools.php>.
- [16] F. Glorius, G. Altenhoff, R. Goddard, C. Lehmann, *Chem. Commun.* **2002**, 2704.
- [17] a) B. M. Trost, M. G. Organ, G. A. O'Doherty, *J. Am. Chem. Soc.* **1995**, *117*, 9662; b) P. E. Blöchl, A. Togni, *Organometallics* **1996**, *15*, 4125; c) P. Dierkes, S. Ramdeehul, L. Barloy, A. Cian, J. Fischer, P. C. J. Kamer, P. W. N. M. van Leeuwen, J. A. Osborn, *Angew. Chem.* **1998**, *110*, 3302; *Angew. Chem. Int. Ed.* **1998**, *37*, 3116.
- [18] For NMR analysis of Pd-allyl complexes see: a) M. D. K. Boele, P. C. J. Kamer, M. Lutz, A. L. Spek, J. G. de Vries, P. W. N. M. van Leeuwen, G. P. F. van Strijdonck *Chem. Eur. J.* **2004**, *10*, 6232; b) J. Mazuela, A. Paptchikhine, P. Tolstoy, O. Pàmies, M. Diéguez, P. G. Andersson, *Chem. Eur. J.* **2010**, *16*, 620; c) A. Sarkar, M. Nethaji, S. S. Krishnamurthy, *J. Organomet. Chem.* **2008**, *693*, 2097; d) M. Diéguez, O. Pàmies, *Chem. Eur. J.* **2008**, *14*, 3653; e) S. Filipuzzi, P. S. Pregosin, M. J. Calhorda P. J. Costa, *Organometallics* **2008**, *27*, 2949.

- [19] a) M. A. A. Boshala, S. J. Simpson, J. Autschbach, S. Zheng, *Inorg. Chem.* **2008**, *47*, 9279; b) A. Oezbolat, G. von Frantzius, W. Hoffbauer, R. Streubel, *Dalton Trans.* **2008**, *20*, 2674; c) C. Compain, B. Donnadieu, F. Mathey, *Organometallics* **2006**, *25*, 540; d) J. R. Goerlich et al., *Phosphorus Sulfur Silicon Rel. Elements* **1992**, *66*, 223.
- [20] a) For *endo/exo* Pd-allyl complexes, see also: M. Kawatsura, Y. Uozumi, M. Ogasawara, T. Hayashi, *Tetrahedron* **2000**, *56*, 2247; b) J. Vázquez, B. Goldfuss, G. Helmchen, *J. Org. Chem.* **2002**, *67*, 641; c) M. Kollmar, B. Goldfuss, M. Reggelin, F. Rominger, G. Helmchen, *Chem. Eur. J.* **2001**, *7*, 4913; d) M. Kollmar, H. Steinhaugen, J. P. Janssen, B. Goldfuss, S. A. Malinovskaya, J. Vázquez F. Rominger, G. Helmchen, *Chem. Eur. J.* **2002**, *8*, 3103.
- [21] a) M. Perez-Rodriguez, A. A. C. Braga, A. R. de Lera, F. Maseras, R. Alvarez, P. Espinet *Organometallics* **2010**, *29*, 4983; b) A. G. Sergeev, A. Spannenberg, M. Beller, *J. Am. Chem. Soc.* **2008**, *130*, 15549; c) S. Teuber Henriksen, D. Tanner, T. Skrydstrup, P.-O. Norby *Chem. Eur. J.* **2010**, *16*, 9494; d) V. P. Ananikov, D. G. Musaev, K. Morokuma *Eur. J. Inorg. Chem.* **2007**, 5390.
- [22] H. A. Bent *Chem. Rev.* **1961**, *61*, 275.